Femtosecond photoelectron imaging of pyridazine: S_1 lifetime and $(3s(n^{-1}),3p(n^{-1}))$ Rydberg state energetics

Yoshiteru Matsumoto[a)]
Institute for Molecular Science, Myodaiji, Okazaki 444-8585, Japan

Sang Kyu Kim[b)]
Department of Chemistry, Inha University, Incheon 402-751, Republic of Korea

Toshinori Suzuki[c)]
Institute for Molecular Science, Myodaiji, Okazaki 444-8585, Japan and Chemical Dynamics Laboratory, RIKEN, Wako 351-0198, Japan and PRESTO, Japan Science and Technology Corporation, Kawaguchi, Japan

(Received 3 February 2003; accepted 7 April 2003)

The first real-time study on pyridazine in the $S_1(n,\pi^*)$ state is presented. The S_1 state is found to dephase with a time constant of 323 ± 17 ps at its origin, and the electronic dephasing mechanism is attributed to the S_1-S_0 internal conversion. The S_1 lifetime is found to decrease rather sharply as the internal energy increases. The $3s$ (n^{-1}) and $3p$ (n^{-1}) Rydberg states of pyridazine are clearly identified in angle- and energy-resolved photoelectron images obtained in the $(1+2')$ photoionization scheme, providing their respective term values of 5.68 ± 0.03 and 6.28 ± 0.04 eV.
 [DOI: 10.1063/1.1578062]

I. INTRODUCTION

Detailed understanding of electronic deactivation processes is essential for elucidating photo-induced dynamics ubiquitous in chemistry and biology.[1] Although conventional approaches such as fluorescence lifetime and quantum yield measurements provide fundamental information on deactivation processes,[2] direct observation of the nonstationary state is by far more informative for disentangling their complex dynamics. Recently-developed time-resolved photoelectron imaging technique[3–6] is extremely useful in this regard, since it provides the most sensitive and versatile means to probe both internal conversion and intersystem crossing processes through the observation of time-dependent energy and angular distributions of photoelectrons.

Diazabenzenes have received a great deal of attention as benchmark systems for the investigation of electronic dephasing processes.[7–12] In particular, pyrazine is the best-studied molecule of an intermediate case,[7,8,10,11] and it is well accepted now that the optically prepared S_1 pyrazine dephases into T_1 manifolds with a lifetime of ~110 ps. Our previous study on pyrazine by time-resolved photoelectron imaging has firmly established this dynamics by visualizing both the decay of S_1 and buildup of T_1 characters in real time.[4,5] Compared to other members of diazabenzene (pyrazine and pyrimidine), pyridazine has been relatively less studied. Accordingly, there seem to be still debates on many fundamental properties of excited states such as the S_1 state lifetime,[13,14] electronic state assignment for S_2,[13–21] and energetics of low-lying Rydberg states.[18,19,22] Another interesting issue is that although pyrazine dephases mainly to the triplet manifold, it has been suggested that pyridazine dephases down to the ground electronic state.[14] This is an interesting difference. Therefore, application of time-resolved photoelectron imaging to this system seems to be a timely research to gain deeper insight into the photophysics and photochemistry of diazabenzenes. This paper reports the first time-resolved study on the excited states of pyridazine.

II. EXPERIMENT

The experimental apparatus employed in the present work has been described in detail elsewhere.[3–6] Pyridazine purchased from Wako was used without further purification. The sample was heated to 80 °C, mixed with a carrier gas of Ar, and expanded continuously through a pinhole 50 μm in diameter into a vacuum chamber with a stagnation pressure of ~1 atm. The free jet was skimmed into the ionization region through a 1 mm diam skimmer to form a collimated molecular beam. The output (80 MHz, 300 mW) of a Ti:sapphire laser (Coherent, Vitesse) was amplified by a regenerative amplifier (Quantronix, Titan) pumped by a Nd:YLF laser (Qunatronix, model 527) to generate a 1 kHz pulse-train (~1.7 mJ/pulse) centered at 802 nm with a bandwidth of ~13 nm. This laser output was then split into two beams, one of which was used to pump an optical parametric amplifier (Light Conversion, TOPAS) to generate an UV pump laser beam tunable in the 350–390 nm range. The other beam was frequency-doubled in a β-BaB_2O_4 crystal to generate the probe laser beam at 401 nm. Cross-correlation width of the pump and probe laser beams was measured to be ~150 fs. The probe beam was optically delayed with respect to the pump beam using a hollow corner cube on a

[a)]Present address: Himeji Institute of Technology, Hyogo 678-1297, Japan.
[b)]Present address: Department of Chemistry and School of Molecular Sciences, Korea Advanced Institute of Science and Technology (KAIST), Daejeon 305–701, Republic of Korea.
[c)]Author to whom correspondence should be addressed. Electronic mail: toshisuzuki@postman.riken.go.jp

computer-controlled delay stage (Sigma Koki, STM-160). The pump and probe beams were spatially overlapped on the molecular beam.

The molecules were ionized by $(1+2')$ resonance-enhanced multiphoton ionization (REMPI), and the resulting ions or electrons were accelerated in a static electric field and projected onto dual-microchannel plates (MCP) 40 mm in diameter backed by a P20 phosphor screen (Photek, OFD-40). The ion/electron current signals were monitored from the AC component of the electric current through the phosphor screen. The photoelectron images on the phosphor screen were observed through a fiber bundle with a thermoelectrically cooled charge-coupled-device (CCD) camera with 512×512 pixels (Princeton Instruments, TE-CCD). Ion optics and electric fields were adjusted to perform velocity mapping that eliminates the blurring of images due to the spatial volume of the laser-molecular beam interaction region. Raw images were inverse-Abel transformed for obtaining 3D photoelectron scattering distributions.

III. RESULTS AND DISCUSSION

A. Ion transients: Electronic dephasing of the S_1 state

The $(1+2')$ REMPI S_1-S_0 excitation spectrum of pyridazine was taken by monitoring the total parent ion signal while scanning the femtosecond pump laser frequency in the 350–390 nm range. The longest wavelength band at 375.5 nm is attributed to the origin of the $S_1(n,\pi^*)-S_0$ transition from comparison with the literature.[13–21] There has been a long-time dispute about the existence of the second electronic origin at 373 cm^{-1} above the first origin,[14–17,21] and yet it does not seem to be settled down. Here, it is assumed that only a single electronic state is involved in the excitation energy region explored in this work.

In order to examine the decay rate from the S_1 state and its vibrational energy dependence, time-profiles of the ion signals were measured at the origin (375.5 nm) and the vibrational energies of 300, 900, and 1900 cm^{-1}. All the transients exhibit sharp rises and single-exponential decays as shown in Fig. 1. A single exponential function is used to fit the experimental results. The time constant is determined to be 323 ± 17 ps at the origin, while time constants of 235 ± 19, 181 ± 22, and 123 ± 19 ps are obtained at internal energies of 300, 900, and 1900 cm^{-1}, respectively. In the past, two contradictory lifetimes of S_1 pyridazine, 0.3 and 3 ns, have been reported from the fluorescence quantum yield measurement[13] and nanosecond time-resolved transient absorption study,[14] respectively. Our results clearly rule out the latter, suggesting that the nanosecond time-resolved transient absorption study[14] may not be adequate for investigating ultrafast dynamics such as the singlet dephasing process though it should be appropriate for studying slow dynamics like the triplet decay.

As demonstrated in the pyrazine case,[3–6] ionization can occur both from the singlet and triplet manifold. However, all the transients in Fig. 1 show rapid decay of the ionization signal down to nearly zero, implying that S_1 pyridazine dephases into an electronic state that is hardly ionized. In the previously reported ground-state repopulation kinetics study,[14] it was concluded that the S_1-S_0 internal conversion is the major decay channel of the S_1 state with a quantum yield larger than 0.95. If this is the case, it will explain why the ion transients in Fig. 1 do not show any growing component, since photoionization from the ground state is Franck–Condon forbidden at the probe wavelength used in this work. Photodissociation of pyridazine into $N_2+CH_2{=}CH{-}C{\equiv}CH$ fragments has been reported to occur at several thousands of cm^{-1} above the S_1 origin with a quantum yield of ~0.1,[23] which further supports rather efficient internal conversion to the ground state. The S_1 lifetime decreases rather sharply with increasing the internal energy; from 323 ± 17 ps at the origin to 123 ± 19 ps at 1900 cm^{-1} above the origin. This may suggest that the vibrational excitation in the S_1 state promotes internal conversion quite efficiently through the mechanism of vibronic coupling. However, the coupling associated with a nearby S_2 state, if it exists, as an additional channel of the S_1 dephasing process cannot be excluded.

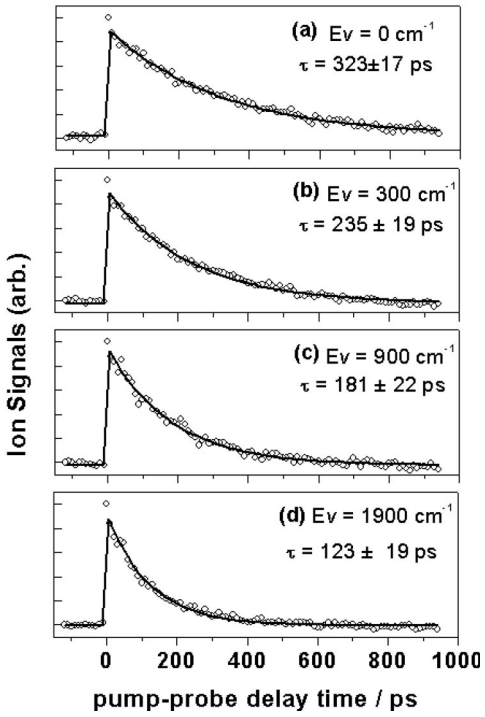

FIG. 1. The ion transient taken at (a) the origin (375.5 nm) with the probe laser at 401 nm. Ion transients taken at the vibrational energies of (b) 300, (c) 900, and (d) 1900 cm^{-1} are also shown.

B. Photoelectron imaging: Energetics of (3s,3p) Rydberg states

Photoelectron images of pyridazine obtained by the $(1+2')$ REMPI with 375.5 nm pump and 401 nm probe at pump–probe delay times of 0, 100, 400, and 800 ps are shown in Figs. 2(a), 2(b), 2(c), and 2(d), respectively. Only two rings are significantly observed. The inner ring corresponding to the lower kinetic energy shows an anisotropic angular distribution, while the more isotropic angular distribution is observed for the outer ring associated with the

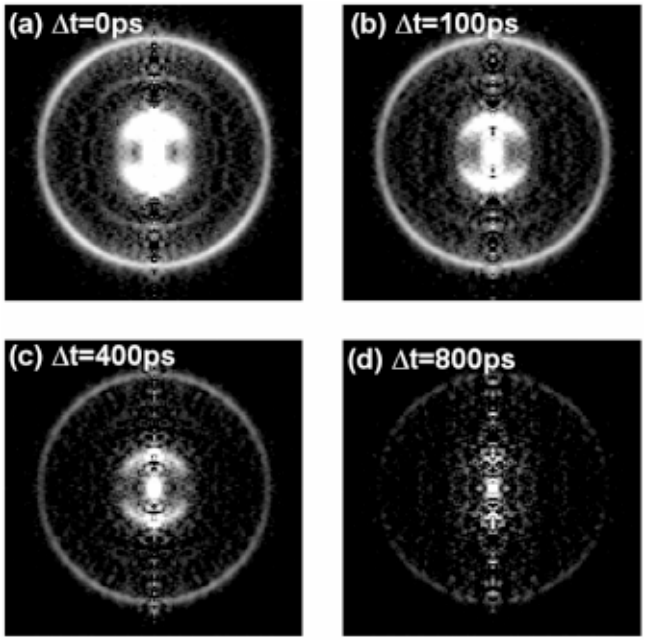

FIG. 2. Photoelectron images of pyridazine taken with the probe at 401 nm at the pump–probe delay times of (a) 0, (b) 100, (c) 400, or (d) 800 ps. The pump laser wavelength was at 375.5 nm.

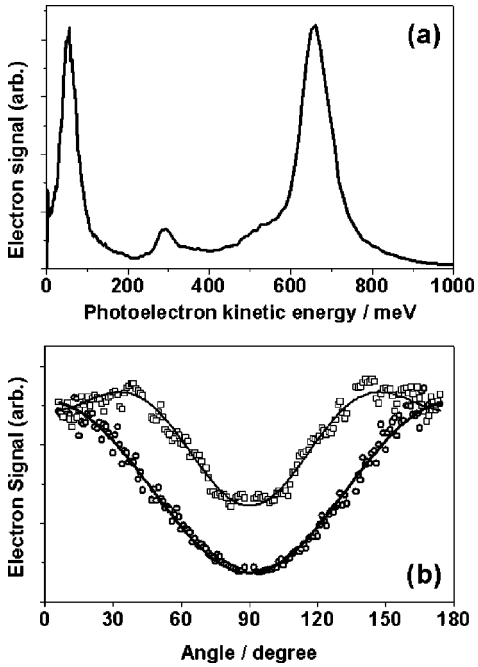

FIG. 3. (a) Photoelectron kinetic energy distribution at pump=375.5 nm and probe=401 nm. Delay time between the pump and the probe pulse was set to 0 ps. The origin for a small peak at ~300 meV is not certain at the present time, although it could be due to vibrational excitation in the photoionziation process via Rydberg states. (b) Photoelectron angular distributions associated with peaks at 60 (○) and 660 meV (□) are shown with the curves obtained by least squares fitting of the equation of $I(\theta) \propto \{1 + \beta_2 P_2(\cos\theta) + \beta_4 P_4(\cos\theta)\}$, where P_k denotes the kth order Legendre polynomial. As for the small peak at 300 meV, see Ref. 24.

higher energy electrons. Both inner and outer rings diminish at longer pump–probe delay times with the same time constant, Fig. 2. The almost identical image pattern had been observed for the $(1+2')$ photoionization of pyrazine,[6] where two rings were attributed to photoelectrons resulting from resonant excitations to the $3s$ and $3p$ Rydberg states as intermediate states in the two-photon ionization process. The difference, however, is that $(1+2')$ REMPI of pyrazine exhibited ionization from the triplet manifold via the triplet $3s$ state. This feature is missing in the present case of pyridazine.

Kinetic energies of photoelectrons are peaked at 60 and 660 meV for inner- and outer-rings, respectively, Fig. 3. The highly anisotropic photoelectron angular distribution (PAD) of the inner ring ($\beta_2 = 1.3 \pm 0.2$, $\beta_4 = -0.0 \pm 0.2$) in Fig. 3 strongly indicates that this is due to photoelectrons in ionization from the $3s$ Rydberg state of pyridazine, since ionization from the s-orbital provides an almost pure p-wave of photoelectron, resulting in the large anisotropy parameter. On the other hand, the outer ring peaked at the kinetic energy of 660 meV shows much less anisotropic PAD, giving $\beta_2 = 0.5 \pm 0.2$ and $\beta_4 = -0.3 \pm 0.2$. Therefore, the outer ring is associated with mixed outgoing partial waves of photoelectrons ejected from the Rydberg $3p$ orbital. The term values, T, of the Rydberg states can be then calculated using the following equation, which is valid for the $(1+2')$ REMPI scheme,[6]

$$\begin{aligned} \mathrm{KE} &= h(\nu_1 + 2\nu_2) - \mathrm{IP} - E_v(\mathrm{Rydberg}) \\ &= T(\mathrm{Rydberg}) + h\nu_2 - \mathrm{IP}. \end{aligned} \quad (1)$$

Here, KE is the kinetic energy of photoelectron, IP is the adiabatic ionization energy, ν_1 is the frequency of the pump laser, ν_2 is the probe laser frequency, and E_v represents the vibrational energy. With the adiabatic ionization energy of 8.706 eV taken from the literature,[18] Rydberg term values associated with kinetic energies of 60 ± 30 (inner-ring) and 660 ± 40 meV (outer-ring) are calculated to be 5.68 ± 0.03 and 6.28 ± 0.04 eV, respectively. These estimated term values are found to be same within experimental uncertainties for different pump wavelengths, validating the above equation.

The term value of 6.306 eV for the $3p$ (n^{-1}) Rydberg state was previously reported by Palmer and Walker[22] from vacuum ultraviolet absorption spectroscopy, while they could not determine the term value for the $3s$ (n^{-1}) state due to spectral overlap of the Rydberg and high-lying valence states. A more recent study using mass-resolved excitation spectra reported the term value of 6.61 eV for the $3s$ (n^{-1}) state,[19] which however is problematic as it is higher than the previously reported energy of 6.306 eV for the $3p$ (n^{-1}) state. This confusion mostly arises from the fact that previous assignments were all based upon only the energies of the Rydberg states. The angular distributions of photoelectrons provide another unambiguous way of assigning the Rydberg states, at least for $l=0$ and others. Judging from their PADs, the states with term values of 5.68 ± 0.03 and 6.28 ± 0.04 eV are ascribed to the $3s$ and $3p$ Rydberg states, respectively. The term value of 6.28 ± 0.04 eV is in excellent agreement with the literature value of 6.306 eV.[18–22] It is interesting to note that the value of 5.68 ± 0.03 eV for the $3s$

(n^{-1}) state is close to 5.50 eV that is roughly estimated by simple algebra from spectroscopically determined energies of 3.30, 4.90, and 7.10 eV for $^1(n,\pi^*)$, $^1(\pi,\pi^*)$, and $(\pi,3s)$ transitions, respectively,[18] since $T[3s(\pi^{-1})] - T[3s(n^{-1})] \approx T[^1(\pi,\pi^*)] - T[^1(n,\pi^*)]$.

IV. SUMMARY AND CONCLUSION

In this work, we report the first real-time study on the photophysics of pyridazine from its S_1 state. Femtosecond-resolved transient monitoring the ion signal provides the lifetime of 323 ± 17 ps for the S_1 pyridazine origin. It is found that the lifetime decreases rather sharply as the vibrational energy increases. The electronic dephasing mechanism of S_1 pyridazine is apparently quite different from the other two diazabenzenes. Namely, while the S_1 state is well known to dephase via the S_1-T_1 intersystem crossing process in both pyrimidine and pyrazine, the main S_1 decay mechanism of pyridazine seems to be the S_1-S_0 internal conversion. This peculiar behavior of pyridazine as a member of diazabenzenes is subjected to further experimental and theoretical studies. Energy and angular distributions of photoelectrons, ejected by the $(1+2')$ REMPI scheme using 375.5 and 401 nm as pump and probe, respectively, clearly reveal $3s$ (n^{-1}) and $3p$ (n^{-1}) Rydberg states of pyridazine, providing their respective term values of 5.68 ± 0.03 and 6.28 ± 0.04 eV. The photoelectron imaging technique is proven to be extremely useful in accurate Rydberg state assignments of pyridazine, which had been vaguely made in previous other studies.

ACKNOWLEDGMENTS

One of the authors (S.K.K.) thanks the Institute for Molecular Science and the Ministry of Education, Culture, Sports, Science and Technology of Japan for financial supports to Japan–Korea binational collaboration program.

[1] P. Avouris, W. M. Gelbart, and M. A. El-Sayed, Chem. Rev. **77**, 793 (1977).
[2] E. K. C. Lee, Adv. Photochem. **121**, 1 (1980).
[3] T. Suzuki, L. Wang, and H. Kohguchi, J. Chem. Phys. **111**, 4859 (1999).
[4] L. Wang, H. Kohguchi, and T. Suzuki, Faraday Discuss. **113**, 37 (1999).
[5] M. Tsubouchi, B. Whitaker, L. Wang, H. Kohguchi, and T. Suzuki, Phys. Rev. Lett. **86**, 4500 (2001).
[6] J. K. Song, M. Tsubouchi, and T. Suzuki, J. Chem. Phys. **115**, 8810 (2001).
[7] A. Frad, F. Lahmani, A. Tramer, and C. Tric, J. Chem. Phys. **60**, 4419 (1974).
[8] F. Lahmani, A. Tramer, and C. Tric, J. Chem. Phys. **60**, 4431 (1974).
[9] I. Yamazaki, T. Murao, T. Yamanaka, and K. Yoshihara, Faraday Discuss. Chem. Soc. **75**, 395 (1983).
[10] J. L. Knee, F. E. Doany, and A. H. Zewail, J. Chem. Phys. **82**, 1042 (1985).
[11] P. J. de Lange, K. E. Drabe, and J. Kommandeur, J. Chem. Phys. **84**, 538 (1986).
[12] D. Zhong, E. W.-G. Diau, T. M. Bernhardt, S. D. Feyter, J. D. Roberts, and A. H. Zewail, Chem. Phys. Lett. **298**, 129 (1998).
[13] A. E. W. Knight and C. S. Parmenter, Chem. Phys. **15**, 85 (1976).
[14] P. L. Holt, J. I. Selco, and R. B. Weisman, J. Chem. Phys. **84**, 1996 (1986).
[15] A. D. Jordan and C. S. Parmenter, Chem. Phys. Lett. **16**, 437 (1972).
[16] E. Ueda, Y. Udagawa, and M. Ito, Chem. Lett. **1981**, 873.
[17] J. Wanna and E. R. Bernstein, J. Chem. Phys. **86**, 6707 (1987).
[18] K. K. Innes, I. G. Ross, and W. R. Moomaw, J. Mol. Spectrosc. **132**, 492 (1988).
[19] C. F. Dion and E. R. Bernstein, J. Chem. Phys. **103**, 4907 (1995).
[20] H. Li and W. Kong, J. Chem. Phys. **109**, 4782 (1998).
[21] G. Fischer and P. Wormell, Chem. Phys. Lett. **257**, 1 (2000).
[22] M. H. Palmer and I. C. Walker, Chem. Phys. **157**, 187 (1991).
[23] J. R. Fraser, L. H. Low, and N. A. Weir, Can. J. Chem. **53**, 1456 (1975).
[24] It is interesting to note that the peak at ~300 meV in Fig. 3(a) does energetically correspond to the state observed by two-photon absorption spectroscopy, in which the state has been assigned to the $3s$ Rydberg state: see J. G. Phillis, J. Mol. Spectrosc. **155**, 215 (1992).